# IFITM3 as a Potential Mechanism for Cyr61 Mediated Inhibition of Oncolytic Virotherapy

Undergraduate Honors Thesis

Presented in Partial Fulfillment of the Requirements for the Degree Bachelor of Science with Distinction in the School of Allied Medical Professions of The Ohio State University

Sean L. Boone

Undergraduate Biomedical Science Major
School of Allied Medical Professions
The Ohio State University

2011

Thesis Committee:
Dr. Balveen Kaur, Ph.D., Adviser
Dr. Bruce Biagi, Ph.D.
Dr. Margaret H. Teaford, Ph.D

# Abstract

Oncolytic virus therapy (OV therapy) exploits naturally occurring or genetically modified viruses to kill cancer cells by lytic destruction. Cysteine-rich protein 61 (Cyr61) has been found to be upregulated by OV infection. Cyr61 was found to inhibit OV infection when using a transient transfection model and when using a tetracycline inducible Cyr61 expression model. In vivo studies using the tetracycline inducible cell lines have shown an inhibition of infection with both subcutaneous and intracranial models. Expression was verified in vitro and in vivo using Western blot. Interferon-induced transmembrane protein 3 (IFITM3) was found to be upregulated in the presence of high levels of Cyr61. As IFITM3 has been previously shown to inhibit the influenza A virus, filoviruses, SARS coronavirus and the HIV-1 virus, its upregulation was posited as the potential mechanism for the observed Cyr61 mediated OV inhibition and thus a potential target for the improvement of treatment efficacy. Indeed, IFITM3 protein was found to be upregulated following OV infection by Western blot in several glioma cell lines. In order to test the effect of IFITM3 on infection, U87, Ln229 and U251T2 cells transiently transfected with IFITM3 protein were infected with an oncolytic herpes simplex virus (HSV-1) harboring a luciferase reporter transgene under an immediate early promoter. Viral quantification was performed by quantifying luciferase activity, normalized to GAPDH protein concentration. No inhibition of OV

infection upon increased IFITM3 levels was noted in any cell line. Therefore, it was concluded that IFITM3 is unlikely to be a mediator of OV therapy inhibition or a target for treatment efficacy improvement.

# Acknowledgements

I would like to thank Dr. Kaur for her mentorship and guidance. It has been a privilege to work within her lab, and with all the people of the Dardinger Laboratory. My time spent researching has been a defining facet of last three years at Ohio State University and has been extremely rewarding. I would also like to thank Amy Haseley, Jason Hardcastle, Nina Dmitrieva and Jeffery Wojton for their support, advice and patience. I have learned much in my time working with Ms. Haseley, and would not be where I am now without her constant assistance and counsel.

I would like to thank Dr. Bruce Biagi and Lori Martenson for all of their assistance and support throughout my college career. I would also like to thank Dr. Biagi, Dr. Kaur, and Dr. Teaford for their donating their time to be committee members and allowing me to defend my thesis project.

# Vita

Sean Logan Boone was born in Seattle, Washington. After graduating high school from Marmion Academy, Aurora, Illinois in 2007, he entered The Ohio State University in Columbus, Ohio. He will be graduating in the spring of 2011 and plans to attend medical school in the fall of 2011.

**Field of Study:**

Major Field: Biomedical Science Major in the School of Allied Medical Professions

Minors: Philosophy, Neuroscience

# Table of Contents

# List of Figures and Tables

# Chapter 1: Introduction

## Glioblastoma Multiforme (GBM)

The most frequently occurring[1] of all brain cancers is glioblastoma multiforme, which the World Health Organization designates as a grade IV astrocytoma. GBM is marked by the presence of small necrotizing regions surrounded by anaplastic cells and is highly motile[2]. This motility leads to both local infiltration and diffuse spread throughout the brain. Another feature of GBM is a high degree of angiogenesis. This angiogenesis feeds tumor growth and is strongly linked to both malignancy[2] and the exponential growth phase of tumors. Angiogenesis has also been shown to suppress immune system recognition of the tumor[3]. Glioblastoma may arise de novo or from a preexisting lower grade glioma and is also one of the most fatal and refractory cancers, with a median time to progression of six months[1] and median standard of care survival of 12-14 months[2]. Current treatments consist of a combination of radiation, surgical resection, and chemotherapy. However, these treatments just add months to the median survival, and <5% of patients survive 5 years[2]. These mortality statistics have not changed much in 50 years and these tumors have resisted[1] innovations in surgery, radiotherapy and chemotherapy. One cause of the difficulties in treatment is the high motility of GBM. As it is spread throughout the brain, complete surgical resection is impossible and the intact blood

brain barrier of healthy regions prevents chemotherapeutic drug access[2]. The poor prognosis of GBM patients necessitates the development of new therapeutic options.

## Oncolytic Virotherapy (OV Therapy)

The idea of treating cancer with viruses is not a new one, as spontaneous tumor regression following viral sickness or rabies vaccination was noticed in 1904[1]. Multiple studies were done in the intervening years, but the most successful might be the 1956 National Cancer Institute study[4] where nearly half of patients experienced tumor regression after wild-type adenovirus treatment. However, this regression was quickly followed by progression, and the investigations were abandoned when a survival benefit was not observed. With modern genetic methods of virology, oncolytic virotherapy has undergone a recent resurgence. Many clinical trials have begun, and recently a Phase III trial[5] demonstrated OV therapy's efficacy as a treatment for squamous cell carcinoma. Gene deletion and modification have minimized toxicity by allowing OVs to only replicate in tumor cells[6,7]. This has permitted many different attenuated viruses to be utilized as OV treatments, and arguably the most favored are reoviruses, adenoviruses and herpes simplex virus (HSV) -1 [8].

HSV-1 is uniquely suited as an OV therapy for brain cancer, as it is non-integrating, well studied, has room for gene addition, specifically targets neural cells, and toxicity can be treated with existing antivirals. Gene addition is particularly important, as this allows for greater therapeutic potential. For example, prodrug activating genes have been included in oncolytic HSV[9]. Oncolytic HSV-1 has also

been used in clinical trials which have shown it to be minimally toxic[10] and in animal trials which have shown an improvement in survival[11] in a glioblastoma multiforme model. This low toxicity arises from two modifications generally made in oncolytic HSV that render it avirulent in the CNS but proliferative in neoplastic cells[1]. One of these modifications has the added benefit of hypersensitizing the virus to treatments such as acyclovir[12]. Although oncolytic HSV is safe, human clinical trials have not been very successful. A few problems have been proposed that might contribute to this lack of efficacy. First, viral spread from the initial area of injection is limited, which prevents effective treatment. One possible solution to this involves the viral production of enzymes degrading the extracellular matrix proteins that inhibit viral diffusion. Attenuation of the virus to improve safety has also limited its replicative ability and the immune system's clearance of the virus decreases infection. The reintroduction of deleted genes under cancer specific promoters increases viral proliferation while still maintaining safety[13].

**Relevance of OV therapy to GBM treatment**

As current therapies have not improved survival beyond a few additional months, a new therapy is essential for survival improvement. OV therapy offers a number of benefits over conventional treatments. As a highly targeted treatment, OV therapy promises the potential of low toxicity and minimal side effects. Radiation and chemotherapy are notorious for their toxic side effects, as both damage normal cells as well as tumor cells. Surgical resection, due to the invasive nature of GBM, either risks removing healthy tissue and creating deficits or leaving tumor behind and failing

to prevent mortality. Another potential benefit of OV therapy is the potential to reach cells beyond the main tumor mass. Another potential benefit of OV therapy is its ability to provide targeted gene therapy. Anti-angiogenic compounds[11] and prodrug converting enzymes[8] have both been included in OV therapy, increasing efficacy and survival in animal models.

## Cysteine-rich, Angiogenic Inducer, 61 (Cyr61) and OV Therapy

Cyr61 is a human 44 kDa protein found intracellularly and secreted into the extracellular matrix. It has been found to be tumorigenic[13] and angiogenic[14]. This angiogenesis is brought about through $\alpha_v\beta_5$ integrin activation. Upon OV therapy Cyr61 has been found to be upregulated[15], as seen in Figure 1. Unpublished results in the Kaur lab have shown that the induction of Cyr61 inhibits oncolytic HSV infection, promotes angiogenesis, aids tumor regrowth and also limits oncolytic virus efficacy. This process of induction and secretion of Cyr61, which acts to inhibit viral infection in nearby cells as seen in Figure 2, offers obvious possibilities as a means for mediating a local antiviral response.

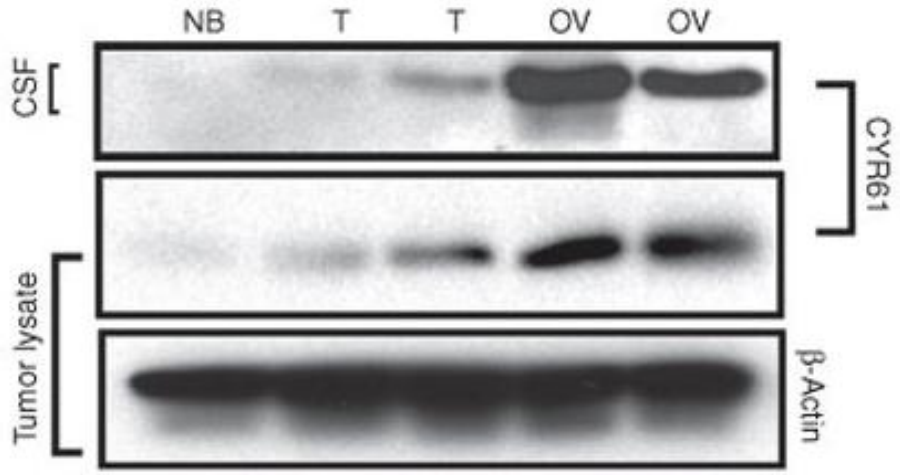


**Figure 1. Cyr61 upregulated after oncolytic virotherapy.**

Rats with intracranial tumors (D74/HveC glioma cells) were treated with hrR3 7 days after tumor implantation. Twenty-four hours after OV treatment, cerebrospinal fluid (CSF) and tumors were harvested from the rats. Cyr61 is seen upregulated following oncolytic virotherapy treatment in both the CSF and in tumor lysates when compared with the PBS treated controls.

(Adapted from Kurozumi et al. Mol Therapy 2008 Aug; 16(8)).

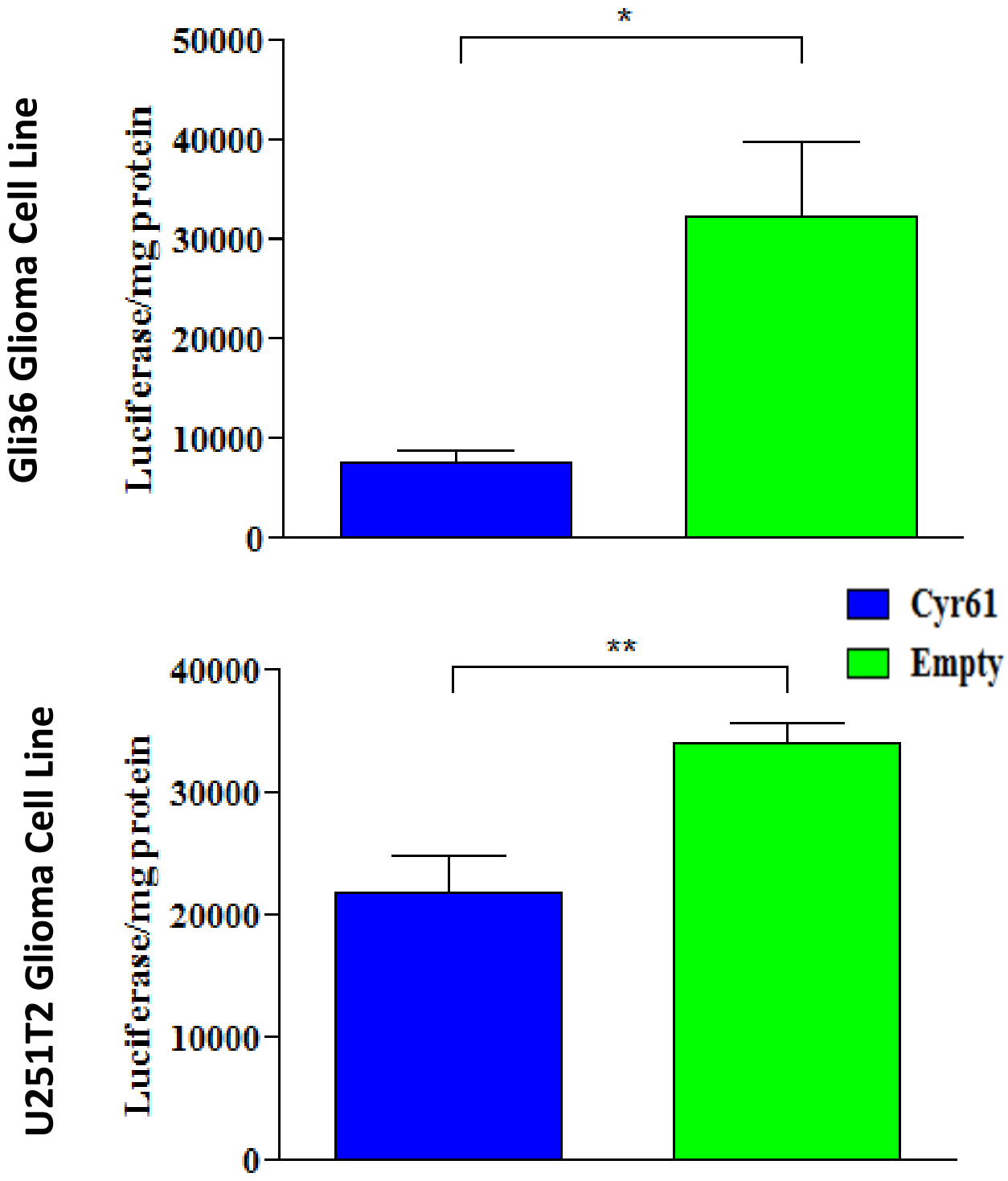


**Figure 2. Inhibition of OV Infection by Cyr61**

Gli36 and U251T2 human glioma cells were transiently transfected with Cyr61 plasmid or empty vector. 24 hours later they were infected with at an MOI 1. Cell lysates were harvested for luciferase activity and normalized to mg of total protein. Cells harboring the Cyr61 plasmid had a significant reduction in luciferase activity as compared to control. Figure adapted from Haseley A et al. Unpublished.

## Interferon-Induced Transmembrane protein 3 (IFITM3)

Interferons were first discovered 50 years ago when they were induced by heat inactivated viral particles[16]. They have since been found to coordinate a large segment of the innate immune response to viral infection[17]. Interferons are commonly used to treat viral diseases such as hepatitis C and have been used as an adjunct to melanoma therapy [18].

IFITM3 has only recently experienced a high level of interest, caused by the discovery of its role in viral inhibition. IFITM3 is a 15 kDa human membrane-bound protein with 2 transmembrane regions. IFITM3, as the name suggests, can be induced by interferon-α and interferon-γ. Interferon-α controls IFITM3's expression by reversible DNA demethylation of its highly regulated core promoter[19]. IFITM3, along with other interferon inducible proteins, is also known as a member of the fragilis gene family. It has been found to play a role in germ cell development and homing[20]. Beyond the developmental role, however, IFITM3 does play a role in innate immunity.

IFITM3 has been found to inhibit West Nile virus, dengue virus, H1N1 influenza, HIV and filoviruses[19, 21]. IFITM proteins are believed to be localized to the late stage endocytic pathway and inhibit a broad range of enveloped viruses[21]. Modification by S-palmitoylation controls IFITM3's membrane clustering and antiviral activity against the influenza virus[22].

## Objectives

Cyr61 was identified as a protein of interest due to its effect on angiogenesis and its upregulation following OV infection. Preliminary studies implied that Cyr61 inhibited viral infection, a novel result, so further analysis was performed. The gol of this project is to validate OV inhibition by Cyr61 and analyze a potential mechanism for it. As IFITM3 was noted in a microarray to be upregulated, and due to its known role in the innate immune response to enveloped viruses, IFITM3 was selected for further analysis. By identifying mechanisms behind viral inhibition, two benefits are accrued: first, one gains a greater understanding of how the body responds to viral infection, with possible treatment potential. Second, one can subvert this process to increase the efficacy of OV therapy.

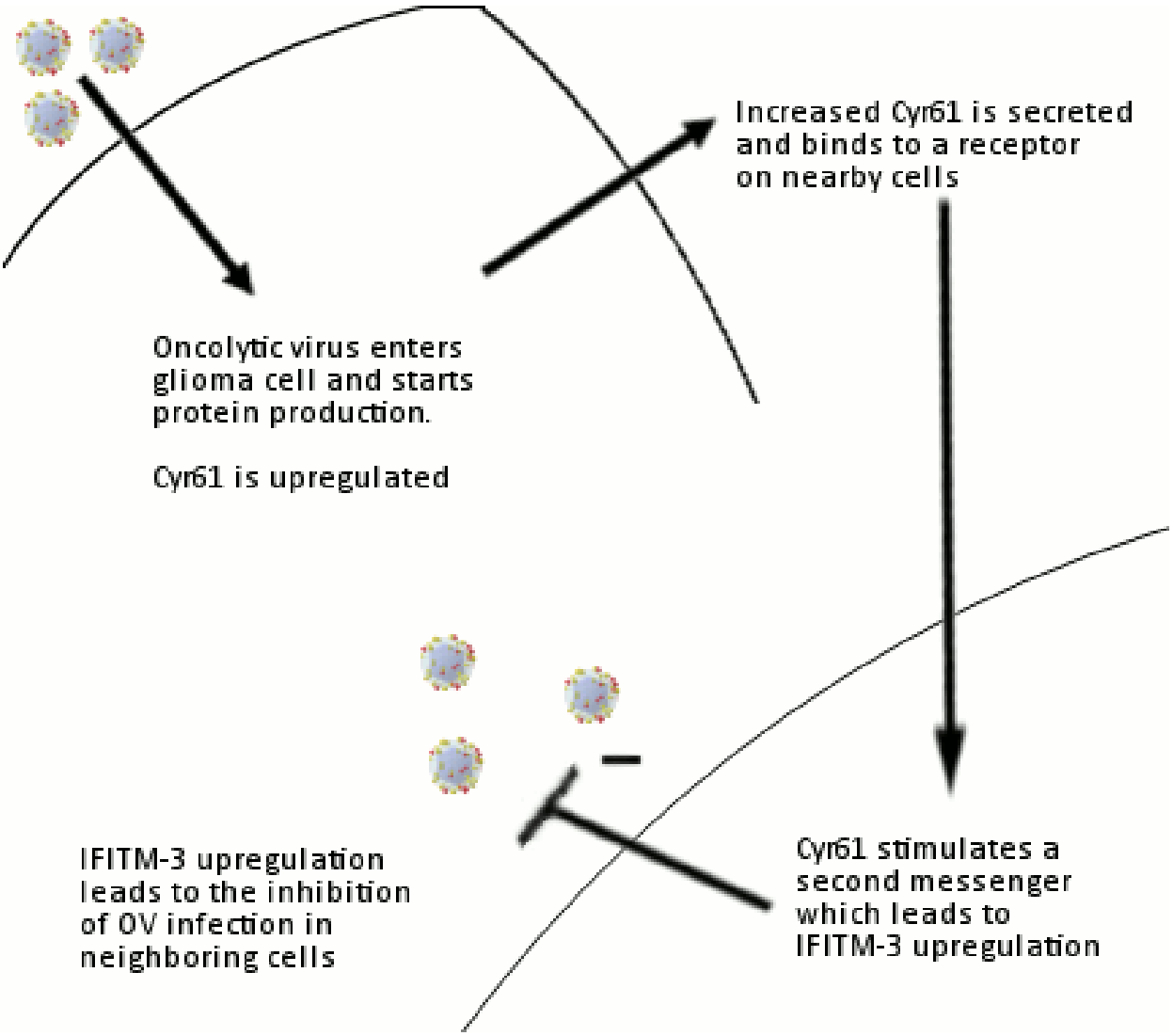


**Figure 3. Proposed mechanism for Cyr61 and IFITM3 mediated inhibition of infection**

It was hypothesized that OV infection leads to Cyr61 production and secretion. This in turn leads to IFITM3 upregulation and IFITM3 then inhibits further OV infection.

# Chapter 2: Material and Methods

## Cells, Viruses and Viral Titration

Human U251T2, Gli36, U343 and U87 cell lines were maintained in Dulbecco's modified minimal essential medium (DMEM) supplemented with 100µg/mL penicillin, 100µg/mL streptomycin, and 10% fetal bovine serum (FBS). Gli36 cells were maintained in selection with 4 µg/mL blasocidin and 2 µg/mL puromycin, but selection was not employed during experimentation.

Two HSV-1 derived oncolytic viruses were used: rHSVQ1, and rQ1-α-Fluc. The genetic structures of both of these viruses and HSV-1 are provided in Figure 4. rHSVQ1 has the gene for the enhanced green fluorescence protein (EGFP) inserted within the UL39 locus of ICP6/RR. This inactivation of ribonucleotide reductase limits replication to within actively cycling cells. The presence of green fluorescence protein (GFP) under the control of the ICP6 locus provides for easy visualization via fluorescent microscopy. In addition, both copies of γ34.5, which is responsible for HSV1's neurovirulence and for host protein shutoff, have been deleted. This virus thus incorporates two methods of glioma targeting. rQ1-α-Fluc is built upon the same backbone as rHSVQ1, but includes the luciferase transgene underneath the HSV-1 IE4/5 promoter (virus courtesy Tarada et al.[23]). Viral stocks were generated and

maintained in Vero cells, derived from green monkey kidneys (American Type Culture Collection, Manassas, VA).

Viral particle quantities were assessed using a viral titration protocol. 10,000 Vero cells are plated per well in a 96 well plate and allowed to adhere overnight. The next day, virus stock is sequentially diluted from $10^{-4}$ through $10^{-10}$. 100µL of each dilution are added to each well and infected for 24±1 h at 37˚C. Using a fluorescent microscope, wells with at least one cell fluorescing in only green, and thus being infected with virus, are marked. The dilution with the nearest to 50% of wells marked is chosen as the dilution. Any wells marked in the next lower dilution are attributed to pipetting error and are added to the number of positive wells in the chosen dilution and divided by the number of wells in the chosen dilution. This percentage is then multiplied by 10 and the dilution factor, and the resultant number is the titer in the units of plaque forming units/milliliter (pfu/mL).

This unit is used to calculate the Multiplicity of Infection (MOI). The probability of a cell absorbing *n* virus particles follows the Poisson distribution, and the infectivity differences can be controlled for by using a functional definition of viral particles. Plaque forming units (pfu) are therefore ideal for use, as this unit only counts the entry of viral particles that can produce GFP and thus are presumed to be functional. An MOI of 2.5 therefore provides 2.5 plaque forming units per cell and therefore the Poisson distribution says that 92% of cells should be infected by at least one viral particle.

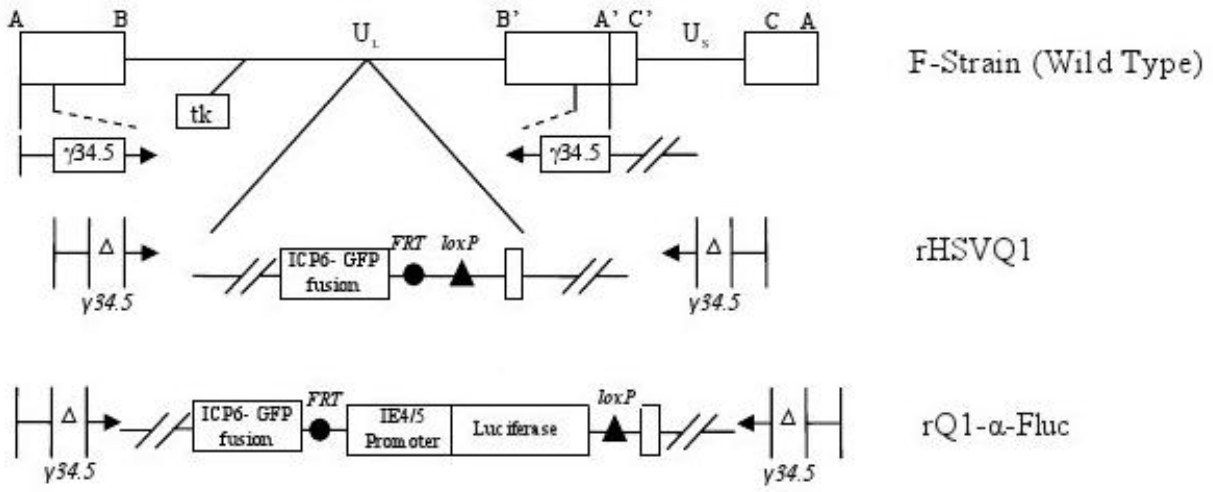


**Figure 4. Genetic Structure of Relevant Viruses**

Viruses were originally created using the HSVQuik method as described previously[23]. Viruses are rendered tumor specific by deleting both γ34.5 copies as well as interfering with ICP6/RR by inserting the genes for GFP and, in the case of rQ1-α-Fluc, the luciferase transgene. The luciferase transgene was inserted under an IE4/5 promoter, as this was previously determined provide optimal luciferase visualization[23].

F-Strain and rHSVQ1 adapted from Hardcastle et. al. Molecular Therapy 2010. 18(2). Q1- α-Fluc graphic was created using his framework.

## Luciferase and the BCA Assay

The Luciferase assay determines the concentration of luciferase transgenetic enzyme by measuring luminescence. Cells were lysed in 1X Cell Lysis Buffer (Promega Corp., Madison, WI ) after a wash in Dulbecco's Phosphate Buffered Saline (Invitrogen). A cell scraper was used to collect the lysate, which was then vortexed, centrifuged to remove cellular debris, and supernatant was frozen. Luciferase activity was measured using the Luciferase Assay System (Promega Corp, Madison, WI). After washing and priming the machine, 80 µL luciferase reagent was automatically added to each 20 µL sample. Luminescence was determined using a Fluorstar Optima reader with negative controls to account for background.

Protein concentration was controlled for using the bicinchoninic acid protein assay (BCA assay). The BCA assay is dependent upon copper ion reduction to produce a colorimetric change. The Pierce® Microplate BCA Protein Assay Kit – Reducing Agent Compatible (Thermo Scientific) was used according to manufacturer's protocol and working reconstitution buffer was not diluted. Protein concentrations were determined by plotting absorbance against a four-parameter quadratic curve. This was created by the FLuostar Optima program by subtracting average absorbance of a blank of 1X Cell Lysis Buffer and finding the best fit line for serially diluted known quantities of BSA. Measurements were taken at 562 nm.

## Western Blots

Immunoblots were performed on cell lysates from indicated cells. Cells were was washed in DPBS and lysed for Western blot in RIPA buffer: 0.1% SDS, 150mM Tris, 150mM NaCl, 1% Nonidet P-40, 0.5% sodium Deoxycholate. If specifically noted, cells were lysed in 1X Cell Lysis Buffer. A cell scraper was used to collect all lysates. 20µL sample was added to 10 µL SDS buffer with 4% 2-mercaptoethanol. After vortexing and centrifugation, samples were heated to 100˚C for 5 minutes, and then samples were vortexed and centrifuged again. Cyr61 protein gels were resolved on 10% SDS-PAGE, and IFITM3 gels were run on a 4-20% SDS-PAGE.

Protein was transferred to PVDF membranes and blocked for at least an hour in blocking buffer (5% non-fat dry milk (LabScientific Inc.) in 0.1% Tween and 1X Phosphate Buffered Saline (PBS-T)) to inhibit non-specific binding between the membrane and nonspecific antibodies. Membranes were incubated in primary antibody for an hour and washed 3x 5 min in PBS-T to remove unbound and nonspecifically bound antibodies. Secondary antibody incubations were 1 hour and were followed by 3x10 min washes in PBS-T and 1x5 min wash in 1xPBS. Visualization was accomplished using enhanced chemiluminescence reagents (GE Healthcare, Pittsburgh, PA), incubated 5 min per manufacturer's protocol. Bands were visualized after exposure and development on hyBlot CL autoradiography film (Dennville Scientific Inc., Metuchen, NJ).

All antibodies were diluted in blocking buffer. **Cyr61** antibody (Novus Biologicals) was diluted 1:750 and a goat anti-rabbit HRP (Dako) diluted at 1:1000 was

used as a secondary. **IFITM3** antibody (Abgent) was diluted 1:200 and the anti-rabbit HRP was again used as a secondary antibody. To control for protein levels, blots were probed for GAPDH, a gene constitutively expressed at high levels and frequently used as a loading control. The **GAPDH** antibody (Abcam) was diluted 1:5,000. The secondary sheep anti-mouse HRP (GE Healthcare) was incubated 1:10,000.

## RNA Preparation and Semi-quantitative Real-time PCR

Cells were harvested with 0.5% trypsin-EDTA, centrifuged to remove cellular debris and the cell pellets were then frozen. Homogenization was accomplished with the QIAshredder (Qiagen) and RNA was isolated using an RNeasy Mini Kit (Qiagen). The Titan One Tube RT PCR System (Roche) was used for semi-quantification per manager's protocol. GAPDH was used as an internal control with relative quantification being expressed as a ratio of the difference in the number of cycles needed for detection at a certain level. Primers were designed using the Primer Express Program (Applied Biosystems).

## Microarray.

Clone 16 cells were incubated with doxycycline for 24 h and harvested using 0.5% Trypsin-EDTA. After centrifugation, RNA was isolated as mentioned previously. Samples, in triplicate, were then submitted to The Ohio State University Microarray Shared Resource Center for microarray analysis using the Affymetrix GeneChip Analysis and analyzed by an affiliated statistician.

## Transfections and Cloning

To create Cy-1, the open reading frame of Cyr61 (amino acids 1-382) was cloned into pcDNA 3.1+myc-His (Invitrogen) for constitutive expression (wt Cyr61) or into pTRE2 (Clontech) for tetracycline-regulated expression (Cyr61mycHisTRE2) using standard techniques. Transient transfections involving IFITM3 were performed using Lipofectamine 2000 (Invitrogen) per protocol from manufacturer. Transient transfections involving Cyr61 were carried out using Lipofectamine reagent and Plus Reagent (Invitrogen) per manufacturer's protocol.

## Animals

All animal experiments were performed in accordance with the Subcommittee on Research Animal Care of the Ohio State University guidelines. Athymic nude mice 6-8 weeks of age were purchased from NCI/NIH. To create subcutaneous tumors, mice were anesthetized and injected in the rear right flank with $4x10^6$ Cy-1 cells. Measurement the tumor were taken using digital calipers and used the ellipsoid volume formula $½xLxW^2$, where the shortest dimension was used as the width[24]. The use of $W^2$ was necessary due to the difficulties inherent when measuring height of a tumor within a living mouse. When subcutaneous tumors reached 2,000 $mm^3$ or per protocol, mice were sacrificed and tumors were collected for analysis.

## Statistical Analysis

Results are presented as mean values ± standard errors of the mean. Statistical analysis was carried out using Students' t-test using Excel 2007. P values of

<0.05 were considered statistically significant. Affymetrix GeneChip was used for gene expression study. Signal intensities were quantified by Affymetrix software, and background correction and quantile normalization were performed to adjust technical biases. Gene expression levels were summarized over probe set using the RMA method, and a filtering method based on percentage of arrays above noise cutoff was applied to filter out low expression genes. A linear model was used to detect differential expression of genes. To improve estimates of variability and statistical tests for gene expressions, a variance shrinkage method was employed, and the significance level was adjusted by controlling the mean number of false positives.

# Chapter 3: Results

## Created Tetracycline-on Cell Lines Demonstrate Cyr61 Induction Upon Doxycycline Treatment

Transient transfections of Cyr61 have been shown to inhibit OV infection (Haseley at al, Unpublished). To validate this we created an inducible cell line. In order to create such a cell line, LN229 was stably transfected with an rtTA expression vector using Lipofectamine and Plus reagent per manufacturer's protocol. This rtTA expression vector, known as Tet-On, is activated by the presence of doxycycline and offers benefits over other modalities of activation. Tet-on is less leaky than the estrogen receptor and is reversible, unlike the Cre and FRT systems. After isolating a Tet-responsive clone, cells were transfected with Cyr61mycHispTRE2 and selected for neomycin resistance (900μg/mL) and tested for Cyr61 induction following doxycycline treatment (1 μg/mL for 24 hrs). Expression of Cyr61 RNA following transfection was determined using a Titan One Tube RT-PCR kit, as previously described. As is seen in Figure 5, treatment with doxycycline (Dox) leads to the expression of Cyr61 in Cy-1 at all examined time points. Having created and verified the Tet-On model, experiments independent of transfection could be performed.

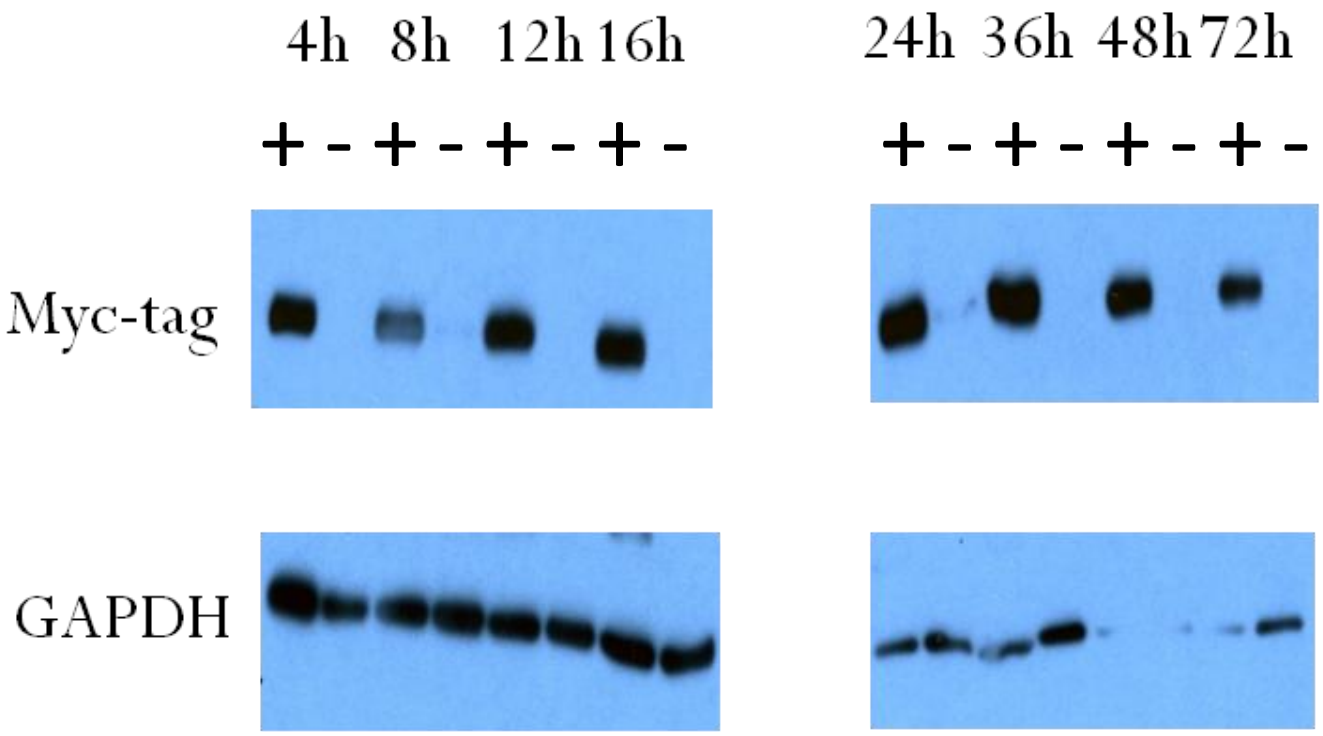


**Figure 5. Cyr61 Induced by Doxycycline at Various Time Points.**

Cy-1 cells were treated with Doxycycline at 1 µg/mL and harvested at various timepoints. GAPDH is used as a loading control. Cy-1 overexpresses Myc-tagged Cyr61 upon doxycycline (dox) treatment from 4 to 72 hours after treatment.

## In Vitro Inhibition of OV infection in Dox Model

With the Tet-On model now available for use, the verification of inhibition was of particular interest. Cy-1 cells were treated with Dox for 24 hours. Cells were infected with rHSVQ1 at a Multiplicity of Infection (MOI) of 2.5 for two hours, and then washed twice with PBS. The high MOI should ensure that almost every cell is infected, as an average of 92% of cells will be infected with at least one viral particle, although this number might be diminished very slightly by the PBS washes. The PBS wash serves to remove any extraneous viral particles still floating, and ensures that the later viral particle count only comes from infected cells. Therefore, all viral particles assayed should be progeny of the first round of infection. 24 hours later, cells were harvested for viral particle titer.

After freeze-thaw cycles, which disrupt the cell and release the viral particles without destroying them, the virus was collected and centrifuged to remove cellular debris. Supernatants were then used to infect Vero cells for 24 hours and viral progeny was determined using viral titration, as described in the methods. As Figure 6 demonstrates, fewer functional viral particles are produced upon dox treatment. This confirms the inhibiton previously seen following transient transfections.

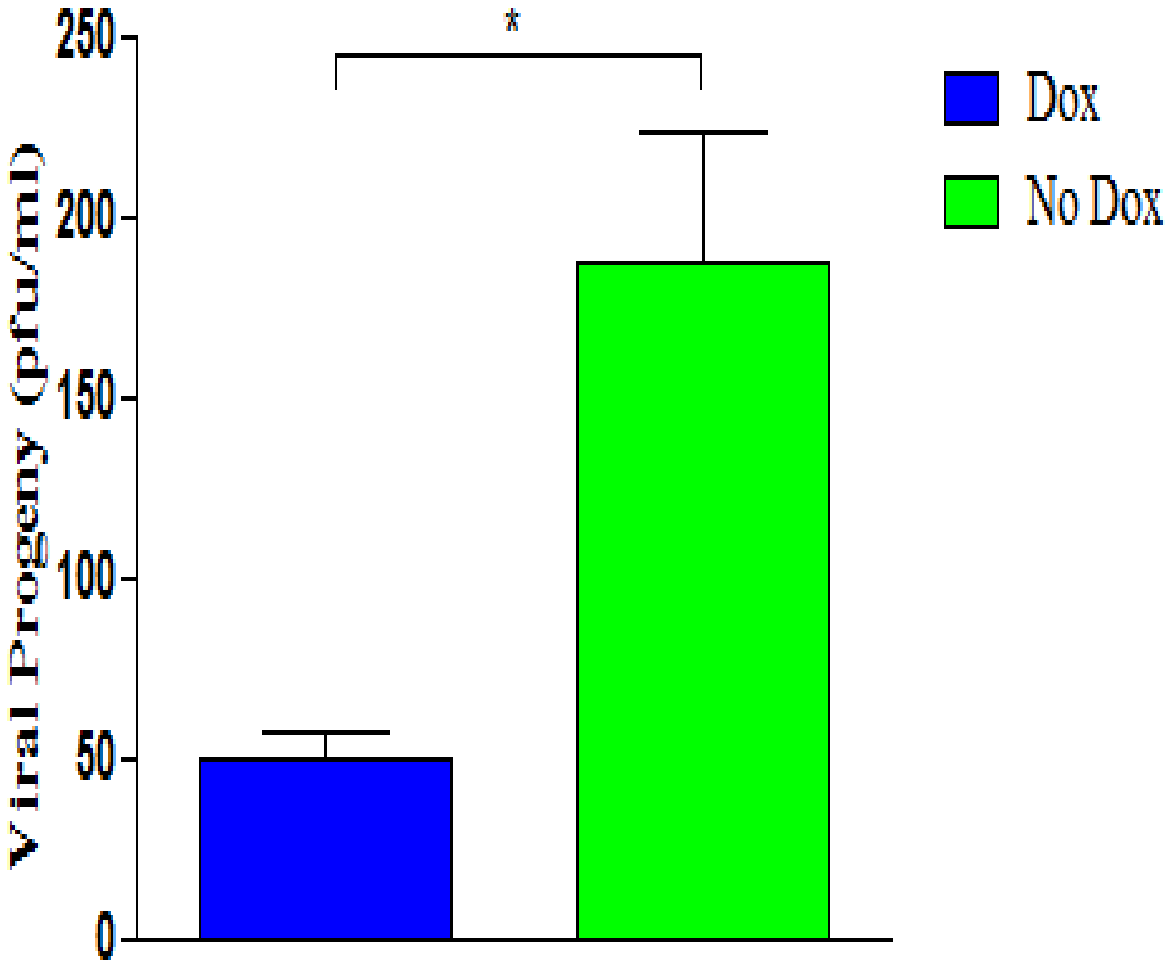


**Figure 6. Tetracycline-Induced Cyr61 Inhibits OV Propagation.**

Cy-1 tet-inducible cells were treated with and without doxycycline (dox) and infected. After 24 hours, virus was collected and the number of viral particles was determined using viral titration as seen in the methods. Cyr61 upregulation, induced by doxycycline treatment, decreased viral progeny.

## Characterization of Dox Model

Having confirmed Cyr61 mediated inhibition, it was important to characterize Cy-1. Conditional expression of Cyr61 in a glioma cell line is novel, and pathways of Cyr61 mediated inhibition of viral infection have not previously been described. Two studies were of particular interest and relevance. First, cells were treated with doxycycline or with normal media. They were then harvested every day for 4 days by fixing with gluteradehyde, and stained with crystal violet. Crystal violet binds to DNA, and thus offers a consistent method of visualization and quantification of cell growth. Quantification was performed using absorbance at $OD_{595}$ and a significant difference was noted between doxycycline treated and untreated cells, as is shown by Figure 7. Cyr61 upregulation also slowed cellular growth.

Cy-1 characterization was also performed in vivo. Mice were implanted with subcutaneous tumors and treated with doxycycline. Dox stock solution was filtered at 0.22µm and diluted to 1mg/mL in sucrose water (5%), as mice resist drinking water with doxycycline if unsweetened. As Figure 8 demonstrates, the growth rate of the tumors was significantly diminished.

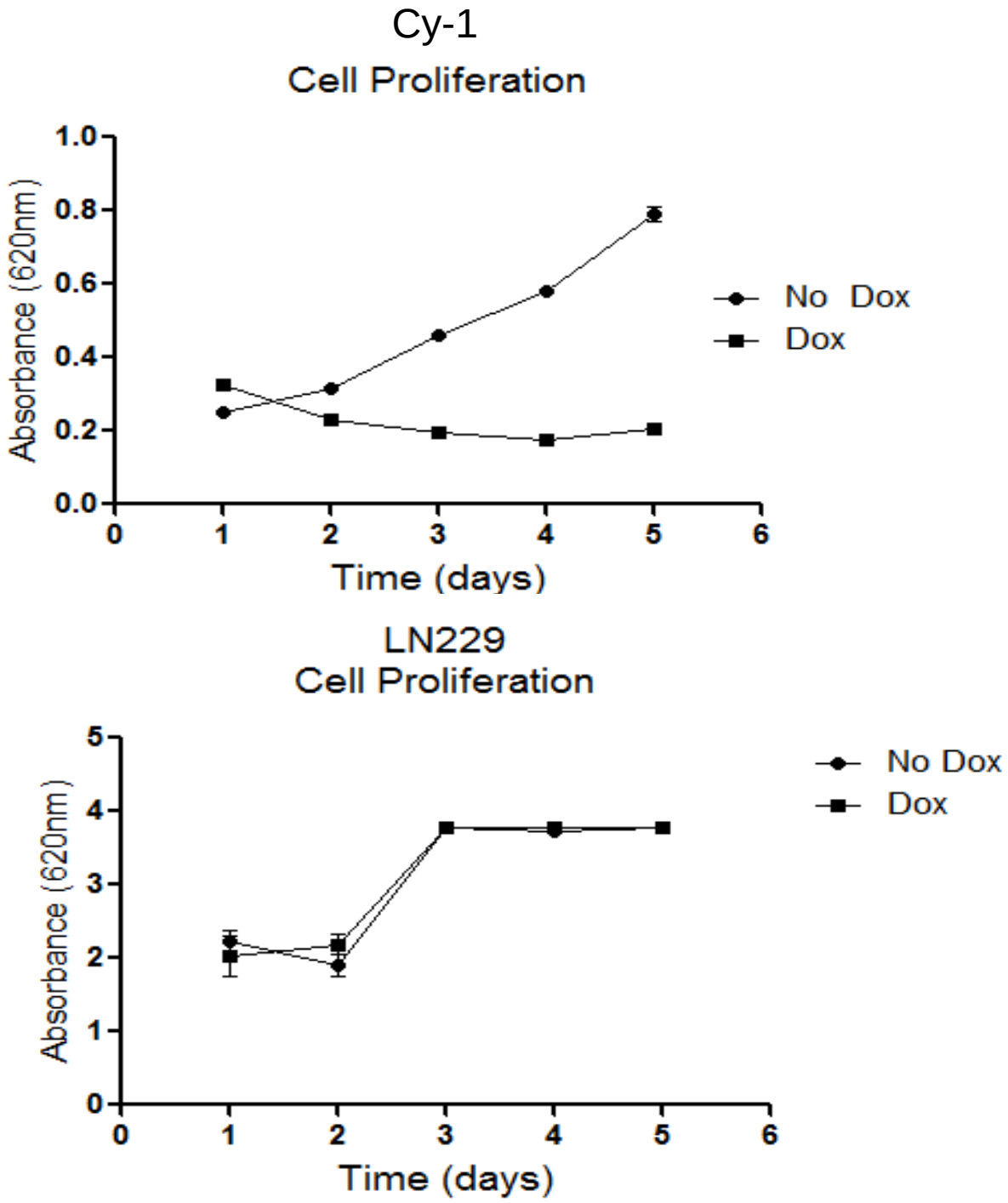


**Figure 7. In Vitro Oxerexpression of Cyr61 Slows Glioma Cell Growth**

Cy-1 and LN229 cells were treated with and without doxycycline and harvested at different time points for cellular density.

Treatment of Cy-1 cells with doxycycline led to decreased growth, while untreated cells grew normally. LN229 was used to ensure that doxycycline itself didn't inhibit growth, as Cy-1 is derived from the transfection of LN229 cells. Dox had no effect upon LN229 growth rates.

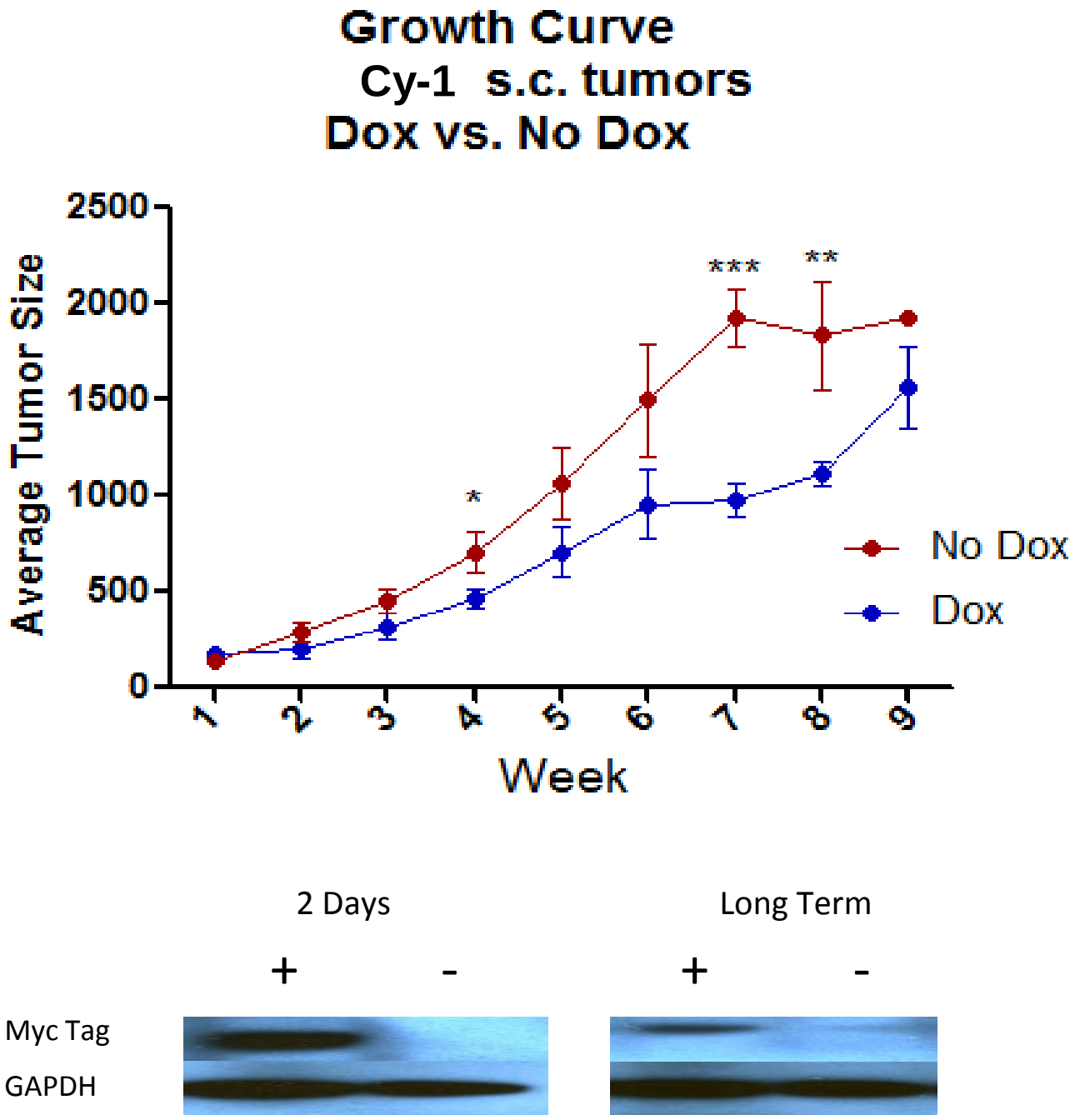


**Figure 8. In Vivo Overexpression of Cyr61 Slows Tumor Growth**

Subcutaneous tumors were created using Cy-1 and mice were treated with doxycycline after tumors reached 100 $mm^3$ and growth was measured weekly. As is seen, doxycycline treated mice showed decreased tumor growth. Western blots of tumor lysates show sustained Cyr61 upregulation with dox treatment.

## IFITM3 Upregulation Shown by Semi-quantitative RT-PCR and Microarray

Having confirmed that Cyr61 inhibits infection using multiple modalities and to identify the mechanism behind infection, we performed a microarray on Cy-1 cells treated with and without doxycycline, as described in previously. IFITM3 was selected as a candidate for further study, due to its recently discovered role in defense against enveloped viruses ($p=2.9x10^{-9}$) and due to the high level of its induction. As seen in Figure 9, IFITM3 expression was significantly increased following induction of Cyr61. This prompted the further review of IFITM3 by semi-quantitative Titan One Tube Assay. Cells were transfected with Cyr61, to see if Cyr61 transfection, in addition to doxycycline treatment, is able to induce IFITM3. Cells were then harvested as discussed previously and the amount of DNA after RT-PCR was qualitatively assessed. In addition, semi-quantitative measurement of the bands was undertaken. As seen in Figure 10, IFITM3 was clearly upregulated following transfection with Cyr61.

This observation strengthened the status of IFITM3 as a candidate gene and prompted a full investigation. If IFITM3 was discovered to mediate Cyr61 induced inhibition of OV infection, this would provide two novel results. First, Cyr61's mechanism of OV inhibition has not been previously described. Secondly, IFITM3's role in either OV therapy or with HSV1 was not previously been examined.

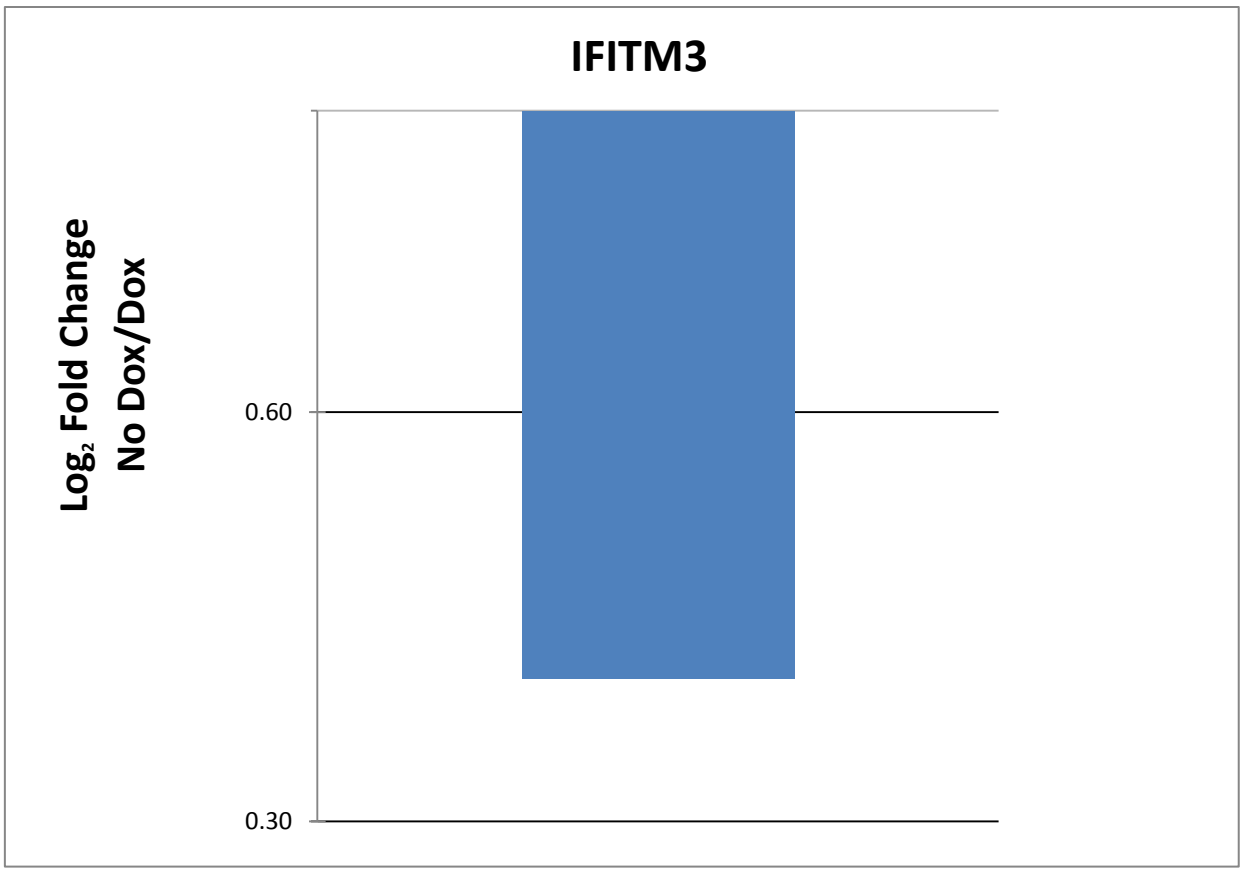


**Figure 9. IFITM3 Levels Higher after Dox Treatment of Cy-1.**

Cy-1 Cells treated with and without doxycycline were subjected to a microarray. The data, after statistical analysis, was in the format of Control/Sample, and thus the number below 1 demonstrates a higher level of IFITM3 in dox treated cells.

IFITM3 was selected as a candidate due to the high significance of increased IFITM3 levels in doxycycline treated cells when compared to untreated cells ($p= 2.9x10^{-9}$). This suggested that Cyr61 upregulates IFITM3.

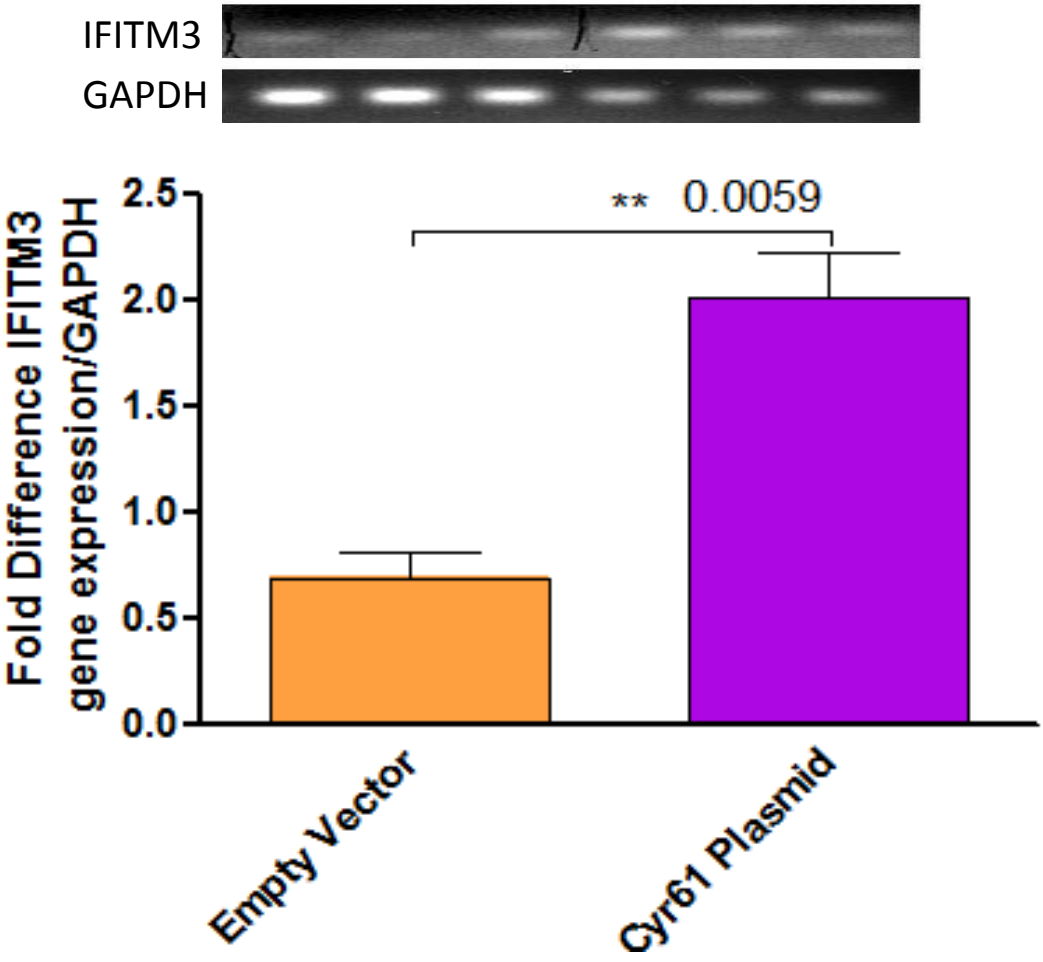


**Figure 10. Titan Semi-quantification RT-PCR Confirms IFITM3 Upregulation Following Cyr61 Transfection.**

U251T2 cells were transfected with Cyr61 and harvested for semi-quantification of IFITM3 RNA levels. After taking into account the loading control, IFITM3 is shown to be upregulated. Above are original bands, and below is quantification of band strength. IFITM3 is shown to be upregulated following Cyr61 transfection (p=0.0059).

## Western Blot of Multiple Cell Lines Shows IFITM3 Upregulation Following OV Infection

Cyr61 induction was sufficient to induce IFITM3 gene expression. Next we investigated whether IFITM3 was induced in glioma cells upon OV infection. To assess this, U87, LN229, Clone 16, U251T2, Gli36 and U343 cell lines were tested to see if IFITM3 was induced after rHSVQ1 infection. $1x10^5$ cells of each cell line besides U87 were plated on a 12 well plate. U87 only had $8x10^4$ cells plated, due to its tendency towards cells forming balls at higher confluencies. The next day, cells were infected at an MOI of 0.1 and untreated samples were harvested. The harvested cells were lysed and analyzed 24 hours after infection by Western blot to check for expression of IFITM3 relative to cellular GAPDH protein levels. Gli36 and Cy-1 showed IFITM3 upregulation subsequent to OV infection. Interestingly, this induction was not observed in U343 or U251T2, as seen in Figure 11. This could be due to issues with sensitivity from the low MOI used. Only 10% of cells are initially infected, but subsequent infection cycles would be expected to infect the majority of cells. The low MOI is used intentionally, as higher MOIs might flood the cells with viral particles, whose numbers might infect many more cells, masking any inhibitory effect.

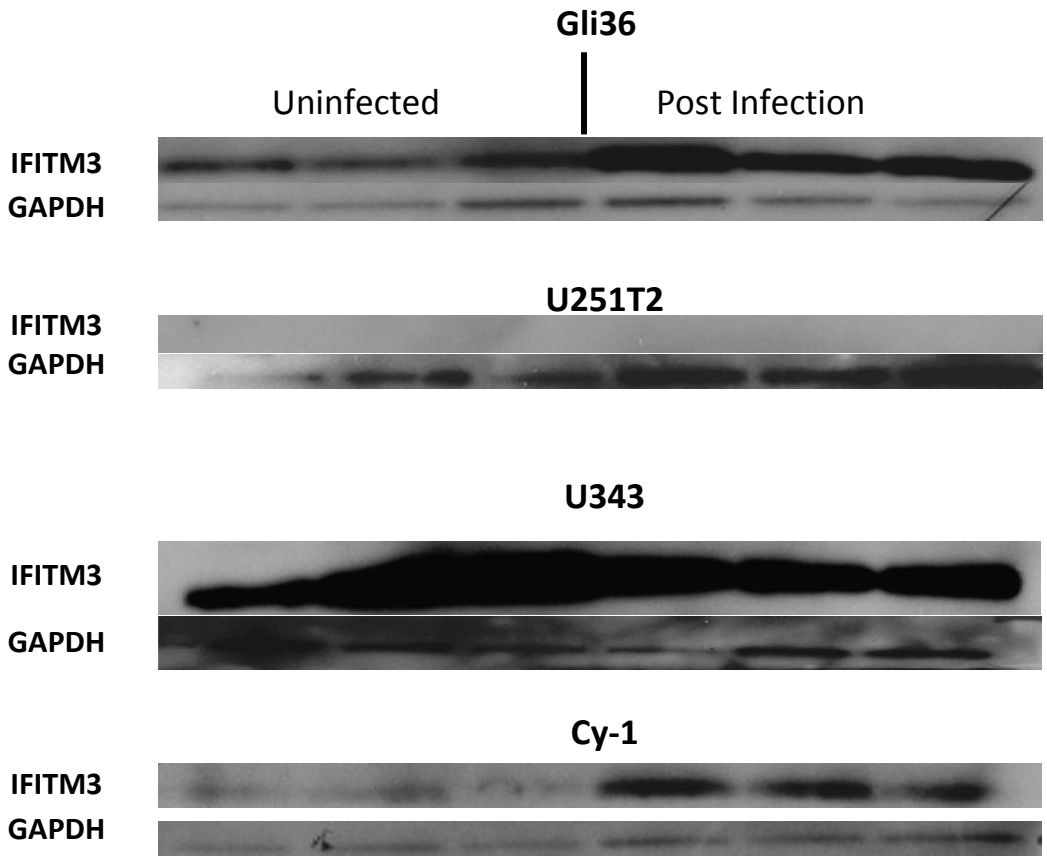


**Figure 11. Western Blot Shows Effects of OV Infection in Different Cell Lines.**

Cells were harvested before and 24 hours after rHSVQ1 infection. Gli36, Cy-1 and U87 show IFITM3 upregulation following infection.

## No Inhibition Shown By Luciferase Following IFITM3 Transient Transfection

The luciferase expressing rQ1-α-Fluc provides an ideal model for examining viral levels following OV infection. As the luciferase transgene is under an immediate-early promoter, cells should produce luciferase very soon after infection and thus luciferase is an indirect marker of viral infectivity. $3x10^5$ cells of LN229 and U87 were transfected with 2μg DNA per well. As Figure 12 demonstrates, no significant difference in infection was observed in LN229 ($p=0.20$) or U87 ($p=0.40$), even with clear upregulation of IFITM3. Having observed no significant difference in OV infection in any cell line, it was deemed unlikely that IFITM3 mediates OV inhibition.

However, one further critique might be raised. It could be that exposure to OVs leads to IFITM3 induction and this increase "masks" the effect of the transfection. All samples for the Western blots verifying transfection were harvested at the time of infection. This is because high IFITM3 levels at the start of infection were desirable to demonstrate that IFITM3 was present to inhibit the virus. To preempt this criticism, the samples harvested for luciferase examination in 1x Cell Lysis Buffer were assessed by Western blot. As is seen in Figure 13, IFITM3 levels 24 hours after infection were similar to those seen at the time of infection. That is, IFITM3 was present in high levels in the transfected cells and at low levels in the control cells. As IFITM3 is minimally present in control cells both at the time of infection and at the time of harvesting, induced IFITM3 was determined to not mask the transfected IFITM3. These results therefore indicate that IFITM3 is not involved in the Cyr61 mediated inhibition of OV therapy in vivo.

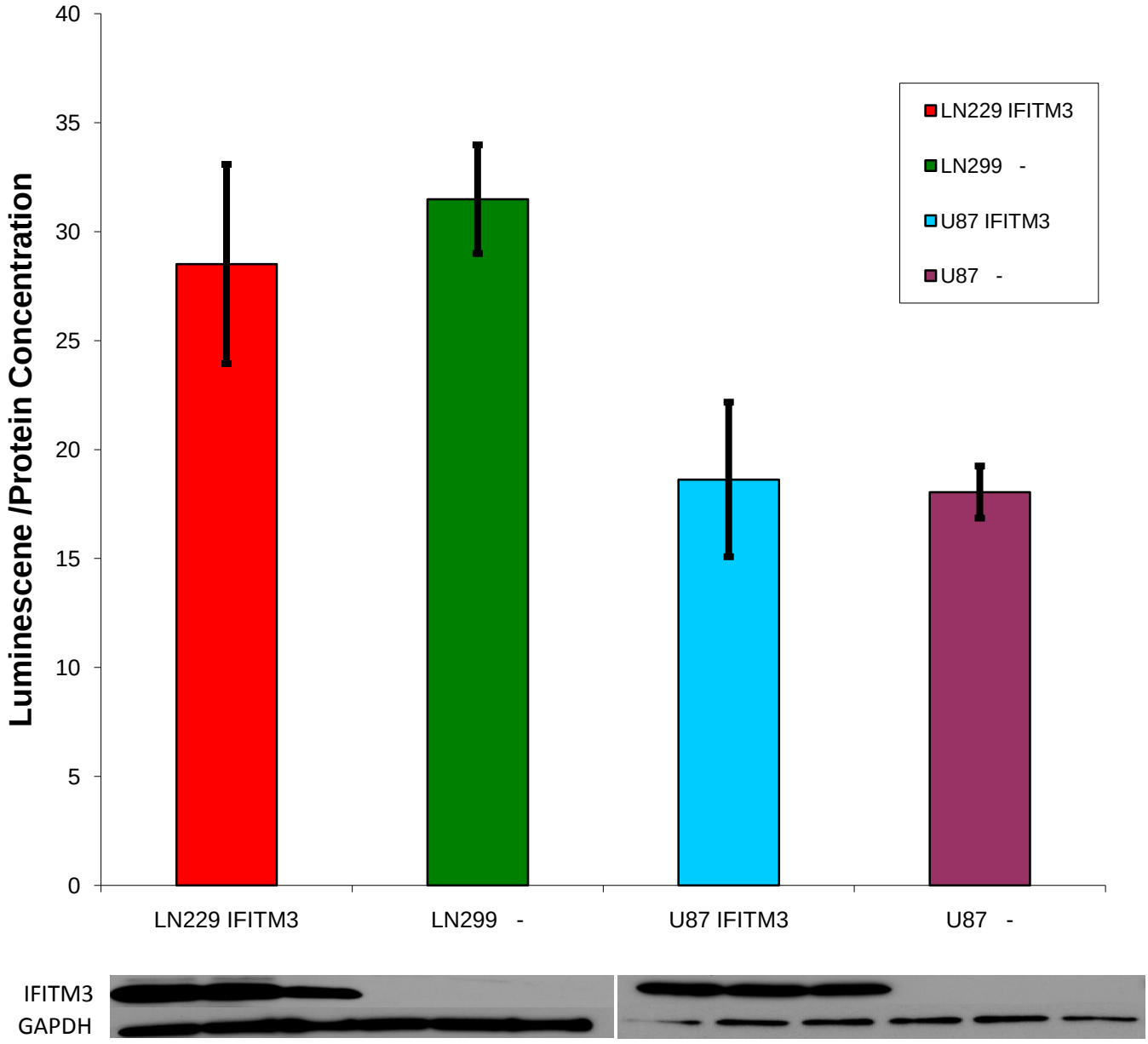


**Figure 12. No Difference in Infection following IFITM3 upregulation in LN229 and U87.**

As U251T2 showed no significant difference in infection, U87 and LN229 were analyzed. Following transfection with the IFITM3 plasmid and infection, LN229 ($p=0.20$) and U87 ($p=0.40$) showed no significant difference in infection. As the Western blots show, IFITM3 is present at high levels in the IFITM3 transfected cells but not in the control transfected cells.

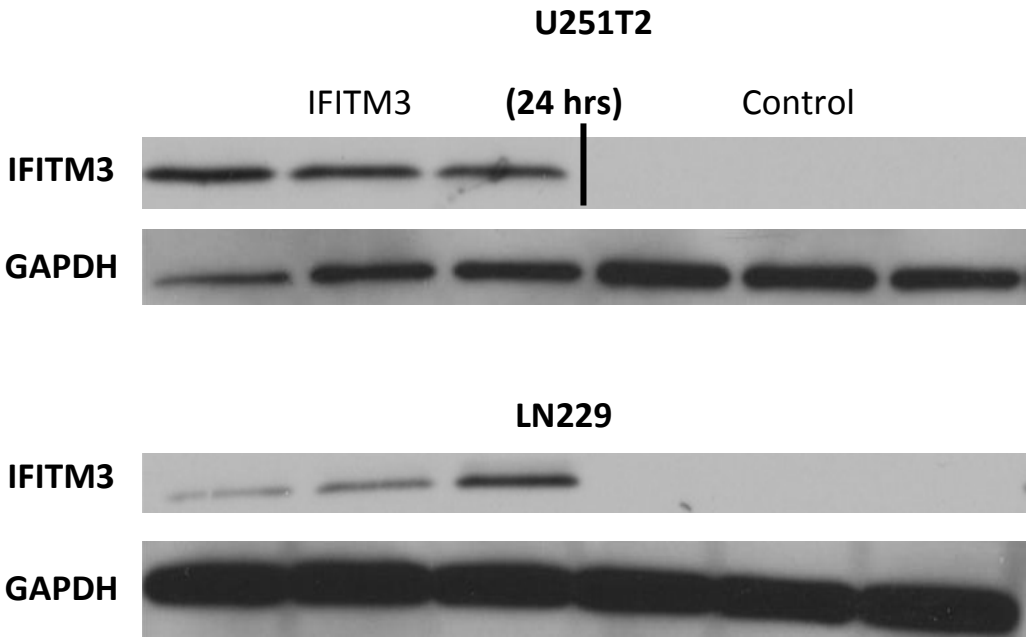


**Figure 13. Transfected Cells Still Express IFITM3 24 Hours After Infection.**

Samples harvested in 1x Cell Lysis Buffer and used for luciferase examination were tested by Western Blot. Cells transfected with IFITM3 and showing no OV inhibition still demonstrate IFITM3 upregulation at the time of harvesting 24 hours after initial infection, and 48 hours after initial transfection.

# Chapter 4: Discussion and Conclusion

OV therapy offers great potential for treating currently incurable cancers, but problems such as the innate defenses against viruses limit clinical application. Here, we have built upon the known induction of Cyr61 and identified, for the first time, that Cyr61 upregulation inhibits OV therapy using transient transfections. A tetracycline inducible model was then created to test inhibition. All modalities confirmed that Cyr61 inhibits OV therapy.

Inhibition obviously limits treatment efficacy, and thus methods aiming to prevent upregulation might improve therapy. One might consider including DNA for the knockdown Cyr61 in infected cells. However, many shRNAs, siRNAs and one shRNA containing virus were all been unable to knockdown Cyr61, so the effort was abandoned (data unpublished). With the most apparent target proving difficult, greater emphasis was put on identifying the mechanism of inhibition. Characterization of tetracycline-inducible clones suggested that the innate antiviral response might be activated by Cyr61.

A microarray and mRNA panel identified that IFITM3 was upregulated when Cyr61 was upregulated. IFITM3 was thus identified as a potential mediator of inhibition, due to its known inhibition of some enveloped viruses, and selected for further evaluation. The evaluation of multiple cell lines demonstrated that OV

infection could induce IFITM3 production, thus providing the possibility that IFITM3 does mediate the observed inhibition. However, upregulation of IFITM3 by transient transfection proved to have no effect upon infection in vitro. This proves the hypothesis that IFITM3 mediates the in vitro observed OV inhibition following Cyr61 upregulation false.

Thus, agents inhibiting IFITM3 are not potential candidates for an adjunct to OV therapy. Ongoing studies aim to identify and understand the mechanisms behind Cyr61 instigated OV inhibition. If identified, this could provide two benefits. First, further analysis of innate immune mechanisms could provide therapeutic targets for more specific immune response modulation with fewer side effects. Secondly, by blocking the identified pathway, the efficacy of OV therapy might be improved.

## References


1. Shah A, Benos D, Gillespie G and Markert J. Oncolytic viruses: clinical applications as vectors for the treatment of malignant gliomas. J of Neuro-Oncology 2003; 65:203-226
2. Groot J and Milano V. Improving the prognosis for patients with glioblastoma: the rationale for targeting Src. J Neurooncol 2009;95:151-163 Folkman J. What Is the Evidence That Tumors Are Angiogenesis Dependent? J Natl Cancer Inst. 1990; 82(1)4-6.
3. Griffioen A. Anti-angiogenesis: making the tumor vulnerable to the immune system. Cancer Immunol Immunother 2008; 57:1553-8
4. Smith R, Huebner R, Rowe W, Schatten W, and Thomas L . Studies on the use of viruses in the treatment of carcinoma of the cervix. Cancer 1956;9:1211–1218.
5. Xia ZJ, Chang JH, Zhang L, Jiang WQ, Guan ZZ, Liu JW, Zhang Y, Hu XH, Wu GH, Wang HQ,Chen ZC, Chen JC, Zhou QH, Lu JW, Fan QX, Huang JJ and Zheng X. Phase III randomized clinical trial of intratumoral injection of E1B gene-deleted adenovirus (H101) combined with cisplatin-based chemotherapy in treating squamous cell cancer of head and neck or esophagus. Ai Zheng, 2004; 23(12) 1666-70.
6. Yu W and Fang H. Clinical Trials with Oncolytic Adenovirus in China. Cur Cancer Drug Targets 2007; 7:141-148
7. Asadi-Moghaddam K and Chiocca EA. Gene- and Viral-Based therapies for Brain Tumors. Neurotheraputics 2009; 6:47-57
8. Bradbury, J. “Oncolytic viral anti-cancer therapy: a magic bullet?” Lancet 2001;357
9. Simpson G and Coffin R. Construction and characterization of an oncolytic HSV vector containing a fusogenic glycoprotein and prodrug activation for enhanced local tumor control. Methods Mol Biol. 2009;542:551-64
10. Kemeny N, Brown K, Covey, A, Kim T, Bhargava A, Brody L, Guilfoyle B, Haag, N, Karrasch M, Glasschroeder B, Knoll A, Getrajdman G, Kowal K, Jarnagin W and Fong Y. Phase I, Open-Label, Dose-Escalating Study of a Genetically Engineered Herpes Simplex Virus, NV1020, in Subjects with Metastatic Colorectal Carcinoma to the Liver 2006, 17(12): 1214-1224 .
11. Hardcastle J, Kurozuki K, Dmitrieva N, Sayers M, Ahmad S, Waterman P, Weissleder R, Chiocca E and Kaur B. Enhanced Antitumor Efficacy of Vasculostatin (Vstat120) Expressing Oncolytic HSV-1. Mol Ther. 2009 Oct 20.
12. Coen DM, Goldstein DJ,Weller SK. Herpes simplex virus ribonucleotide reductase mutants are hypersensitive to acyclovir. Antimicrob Agents Chemother 1989; 33: 1395–1399
13. Tsai M, Bogart D, Castaneda J, Li P and Lupu R. Cyr61 promotes breast tumorigenesis and cancer progression. Oncogene 2002; 21(53):8178-85.

14. Estrada R, Li N, Sarojini H, An J, Lee MJ and Wang E. Secretome from mesenchymal stem cells induces angiogenesis via Cyr61. J Cell Phys 2009; 219(3): 563 – 571.
15. Kurozumi K, Hardcastle J, Thakur R, Shroll J, Nowicki M, Otsuki A, Chiocca EA and Kaur B. Oncolytic HSV-1 infection of tumors induces angiogenesis and upregulates CYR61. Mol Ther. 2008 Aug;16(8):1382-91.
16. Isaacs A, Lindenmann J. 1957. Virus interference. I. The interferon. Proc R Soc Lond B Biol Sci 147(927):258–267.
17. Takaoka A and Yanai H. Interferon Signalling Network in Innate Defense. Cell. Microbio. 2006;8:907-922.
18. Lindnér P, Rizell M, Mattsson J, Hellstrand K, Naredi P. Combined treatment with histamine dihydrochloride, interleukin-2 and interferon-alpha in patients with metastatic melanoma. Anticancer Res. 2004 May-Jun;24(3b):1837-42.
19. Scott R, Siegrist F, Foser S, Certa U. Interferon-Alpha Induces Reversible DNA Demethylation of the Interferon-Induced Transmembrane Protein-3 Core Promoter in Human Melanoma Cells. J Interferon Cytokine Res. 2011 Mar 17
20. Tanaka SS, Yamaguchi YL, Tsoi B, Lickert H, Tam PP. IFITM/Mil/fragilis family proteins IFITM1 and IFITM3 play distinct roles in mouse primordial germ cell homing and repulsion. Dev Cell. 2005 Dec;9(6):745-56.
21. Huang IC, Bailey CC, Weyer JL, Radoshitzky SR, Becker MM, Chiang JJ, Brass AL,Ahmed AA, Chi X, Dong L, Longobardi LE, Boltz D, Kuhn JH, Elledge SJ, Bavari S, Denison MR, Choe H, Farzan M. Distinct patterns of IFITM-mediated restriction of filoviruses, SARS coronavirus, and influenza A virus. PLoS Pathog. 2011 Jan6;7(1)
22. Yount JS, Moltedo B, Yang YY, Charron G, Moran TM, López CB, Hang HC. Palmitoylome profiling reveals S-palmitoylation-dependent antiviral activity of IFITM3. Nat Chem Biol. 2010 Aug;6(8):610-4.
23. K Terada,H Wakimoto, E Tyminski, EA Chiocca and Y Saeki. Development of a rapid method to generate multiple oncolytic HSV vectors and their in vivo evaluation using syngeneic mouse tumor models. Gene Therapy (2006) 13, 705–714
24. Tomayko M and Reynolds CP. Determination of subcutanteous tumor size in athymic (nude) mice. Cancer Chemother and Pharm. Volume 24, Number 3, 148-15
25. Dock G. Rabies virus vaccination in a patient with cervical carcinoma. Am J Med Sci 1904;127:563.
26. Hu J, Coffin R, Ceri D, Graham N, Groves N, Guest P, Harrignton K, James N, Love C, McNeish I, Medley L, Michael A, Nutting C, Pandha, H, Shorrock C, Simpson J, Steiner J, Steven N, Wright D and Coombes Rl. A Phase I Study of OncoVEX$^{GM-CSF}$, a Second-Generation Oncolytic Herpes Simplex Virus Expressing Granulocyte Macrophage Colony-Stimulating Factor. Clin Cancer Res 2006; 12(22).
27. Kambara H, Okano H, Chiocca EA and Saeki Y. An oncolytic HSV-1 mutant expressing ICP34.5 under control of a nestin promoter increases survival of animals even when symptomatic from a brain tumor. Cancer Res. 2005;65(7):2832-9
28. Haseley A, Boone S and Hardcastle J. Unpublished work.

29. Bender F, Whitbeck JC, Lou H, Cohen G and Eisenberg R. Herpes simplex virus glycoprotein B binds to cell surfaces independently of heparan sulfate and blocks virus entry. J Virol. 2005; 79(18):11588-97
30. Grzeszkiewicz TM, Lindner V, Chen N, Lam SC and Lau LF. The angiogenic factor cysteine-rich 61 (CYR61, CCN1) supports vascular smooth muscle cell adhesion and stimulates chemotaxis through integrin alpha(6)beta(1) and cell surface heparan sulfate proteoglycans. Endocrinol. 2002; 143(4):1441-50
31. Interferon-Induced Transmembrane Protein-3 Core Promoter in Human Melanoma Cells. J Interferon Cytokine Res. 2011 Mar 17.